Fusion Engineering and Design 215 (2025) 114961

Contents lists available at ScienceDirect

Fusion Engineering and Design

journal homepage: www.elsevier.com/locate/fusengdes

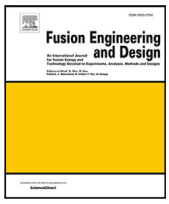

H-Mode density limit disruption avoidance in ASDEX Upgrade, TCV and JET

B. Sieglin [a,*], M. Maraschek [a], A. Gude [a], F. Klossek [a], F. Felici [b], M. Bernert [a], O. Kudlacek [a], A. Pau [b], L. Piron [c], M. Lennholm [d], K. Kirov [d], S. Hongjuan [d], A. Parrott [d], P. Fox [d], O. Sauter [b], C. Stuart [d], C. Ashe [d], A. Huber [e], W. Treutterer [a], the ASDEX Upgrade Team[1], the TCV Team[2], the JET contributors[3], the EUROfusion WPTE Team[4]

[a] Max–Planck-Institute for Plasma Physics, Boltzmannstr. 2, Garching near Munich, 85748, Bavaria, Germany
[b] Ecole Polytechnique Fédérale de Lausanne (EPFL), Swiss Plasma Center (SPC), Lausanne, CH-1015, Switzerland
[c] Dipartimento di Fisica "G. Galilei", Università degli Studi di Padova, Padova, Italy
[d] UKAEA, Culham Campus, Abingdon, OX14 3DB, Oxfordshire, UK
[e] Forschungszentrum Jülich GmbH, Wilhelm-Johnen-Straße, Jülich, 52428, Germany

ARTICLE INFO

Keywords:
Tokamak
Plasma control
Disruption avoidance

ABSTRACT

In recent years a strong effort has been made to investigate disruption avoidance schemes in order to aid the development of integrated operational scenarios for ITER. Within the EUROfusion programme the disruptive H-Mode density limit (HDL) has been studied on ASDEX Upgrade, TCV and JET. This paper presents the results from these studies in the view of the plasma control system (PCS).

The successful migration of disruption avoidance schemes based on direct measurements as well as state space based HDL observers across the devices has been demonstrated. HDL disruption avoidance using continuous control is now routinely available at TCV and ASDEX Upgrade, using both observer types. Exception handling based disruption avoidance has been utilized on all three devices. All three control systems allowed the implementation of the desired schemes with minimal adaptions, implementing the equivalent detection algorithms. Using the same experimental methodology it is confirmed that the XPR/MARFE movement, which is preceding the disruptive HDL, is similar on all three devices. The main difference lies in the associated times scales which increase with machine size. This would be beneficial for large devices, such as ITER and DEMO, since it would give the control system more time to apply the appropriate disruption avoidance action. As actuator auxiliary heating, gas flow and plasma shaping have been successfully demonstrated.

This work gives input for the requirements of future tokamak control systems which should enable the necessary disruption avoidance schemes. All disruption avoidance schemes developed during the studies can be implemented in the ITER PCS with its currently foreseen capabilities.

1. Introduction

Disruptions pose a significant threat for large fusion devices such as ITER and DEMO. The thermal and mechanical stresses they induce onto the device become intolerable if not mitigated [1]. However, even if mitigated, only a limited number of disruptions will be tolerable. Disruption avoidance aims to prevent the plasma to become disruptive via means of active control.

The basic requirements for the implementation of disruption avoidance for a specific disruption path are the following.

- An **observer** needs to be available to the control system to monitor if the plasma and/or plant state are approaching a likely disruption.
- An **actuator** which is capable of changing the plasma state to be non disruptive.

* Corresponding author.
E-mail address: bernhard.sieglin@ipp.mpg.de (B. Sieglin).

[1] See author list of H. Zohm et al. 2024 Nucl. Fusion https://doi.org/10.1088/1741-4326/ad249d.
[2] See author list of H. Reimerdes et al. 2022 Nucl. Fusion **62** 042018.
[3] See author list of E. Joffrin et al. 2019 Nucl. Fusion **59** 112021.
[4] See author list of "Progress on an exhaust solution for a reactor using EUROfusion multi-machines capabilities" by E. Joffrin et al. to be published in Nuclear Fusion Special Issue: Overview and Summary Papers from the 29th Fusion Energy Conference (London, UK, 16–21 October 2023).

https://doi.org/10.1016/j.fusengdes.2025.114961
Received 13 December 2024; Received in revised form 28 February 2025; Accepted 7 March 2025
Available online 18 March 2025
0920-3796/© 2025 The Authors. Published by Elsevier B.V. This is an open access article under the CC BY license (http://creativecommons.org/licenses/by/4.0/).

- A **control logic** to judge and apply the appropriate action to avoid the disruption.

Both continuous control and exception handling, and their combination, have demonstrated the capability to implement disruption avoidance on existing devices [2–10] for various disruption paths.

An open question that remained was the extrapolation and transfer of disruption avoidance schemes in between devices and especially towards larger devices. In order to investigate this, TCV, ASDEX Upgrade and JET have been used in a step ladder approach, implementing disruption avoidance with the available capabilities for the specific device.

There are various causes leading to disruptions [11,12]. As a test case for the investigation the disruptive H-Mode density limit (HDL) has been chosen, since it fulfilled the following requirements on all three devices.

- It is achievable/existent.
- Diagnostics to detect the proximity to the HDL in real time are available to the specific control systems.
- Actuators for the prevention of the HDL are available and controllable in real time.

The actuators that have been tested to implement HDL disruption avoidance on the three devices are the increase of the auxiliary heating power, the reduction of the gas fuelling rate as well as the combination of both.

2. H-mode density limit

The HDL is especially relevant for future fusion reactors in which a high plasma density is desired in order to maximize the fusion gain. It has been extensively studied on various devices [9,13–19]. Empirical [20] and theoretical [21,22] models exists for its description.

The rough outline of an HDL is as follows. As the density is increasing first the plasma stored energy is increasing up to a point where it saturates. If the density is further increased the stored energy gradually starts to decrease. At some point the HL-transition occurs which leads to a strong reduction of the stored energy and density, even if the gas fuelling is increased further. Commonly the HDL is accompanied by a poloidally localized toroidal symmetric phenomenon called X-Point radiator (XPR) [23,24] or Multifaceted Asymmetric Radiation From the Edge (MARFE) [13,14,25,26] which performs a characteristic poloidal movement (Figs. 2 and 3) and ultimately leads to a significant cooling of the confined plasma from the edge. If not reacted on, this induces a loss of confinement or disruption.

It was found on ASDEX Upgrade that the characteristic XPR/MARFE movement away from the X-Point can either start in H- or L-Mode depending on the applied auxiliary heating [9]. It has to be noted that the onset and development of the MARFE depends on the local conditions in the edge of the plasma. The onset of the MARFE might align with density limits, such as the Greenwald density, which are described using global averaged quantities, when core and edge conditions are strongly coupled. However, there can be a considerable discrepancy when this coupling is broken., by e.g. impurities [24,27] and/or strongly peaked core density profiles [28,29].

3. Observers

For the HDL detection two main observers have been developed and implemented on the different devices.

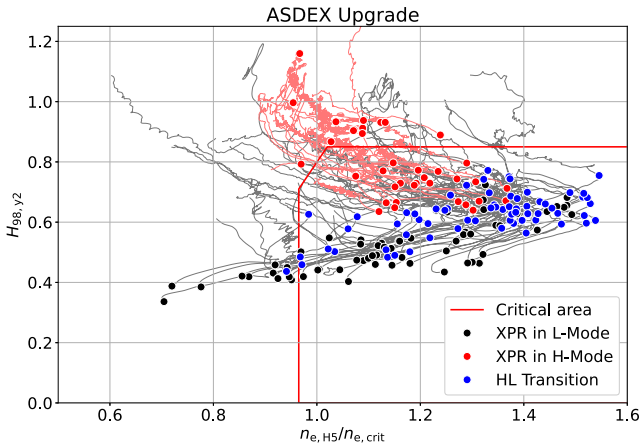

Fig. 1. Trajectories of ASDEX Upgrade HDL disruption avoidance experiments in the HDL state space. The red and black dots mark the start of the movement of the XPR/MARFE away from the X-Point. The blue dots indicate the HL-transition. The red box indicates the empirically defined *critical area* for the HDL [4].

3.1. HDL state space

The first one is an empirical state space [4] defined by the confinement factor $H_{98,y2}$ and an edge electron density fraction f_{crit}.

$$f_{crit} = \frac{n_e}{n_{e,crit}} \tag{1}$$

where n_e is the line integrated edge electron density measured by the DCN interferometer channel H-5 [30]. $n_{e,crit}$ is the empirical description of the line integrated edge electron density at which the HL transition occurs in ASDEX Upgrade [16]:

$$n_{e,crit} = 0.506 \cdot P_{heat}^{0.396} \cdot I_p^{0.265} \cdot q_{95}^{-0.323} \tag{2}$$

where P_{heat} is the auxiliary heating power in MW, I_p the plasma current in MA and q_{95} the safety factor. In this state space a *critical area* [4] (see red box in Fig. 1) has been empirically defined using HL-transitions from previous HDL experiments performed at ASDEX Upgrade.

Fig. 1 shows the trajectories of the disruption avoidance experiments performed in ASDEX Upgrade in the HDL state space. The trajectories are shown up to the time point when the XPR/MARFE started moving away from the X-Point and the disruption avoidance action was triggered. This is marked by red (discharge in H-Mode) and black (discharge in L-Mode) dots. The blue dots mark the HL transition for the discharges where the XPR movement started in L-Mode. It is seen that the *critical area* covers most of the HL transitions.

It has to be noted that at ASDEX Upgrade the critical edge density regression (Eq. (2)) has been performed using the edge line integrated DCN interferometer channel H-5 [30]. Therefore, the critical edge density has to be adapted to the specific diagnostic setup on other devices.

3.2. Direct observation of XPR/MARFE

The XPR/MARFE which occurs during the development of the HDL is observable via bolometry and/or fast photo diodes. An example of an offline reconstruction of the XPR/MARFE movement towards an HDL disruption on ASDEX Upgrade is shown in Fig. 2.

Real time tracking of the XPR/MARFE has been developed on ASDEX Upgrade [9] and successfully used for detachment control [23] and disruption avoidance [9]. In experiments on TCV similar XPR/MARFE behaviour as documented on ASDEX Upgrade is observed. The utilization of the XPR/MARFE observer for disruption avoidance on

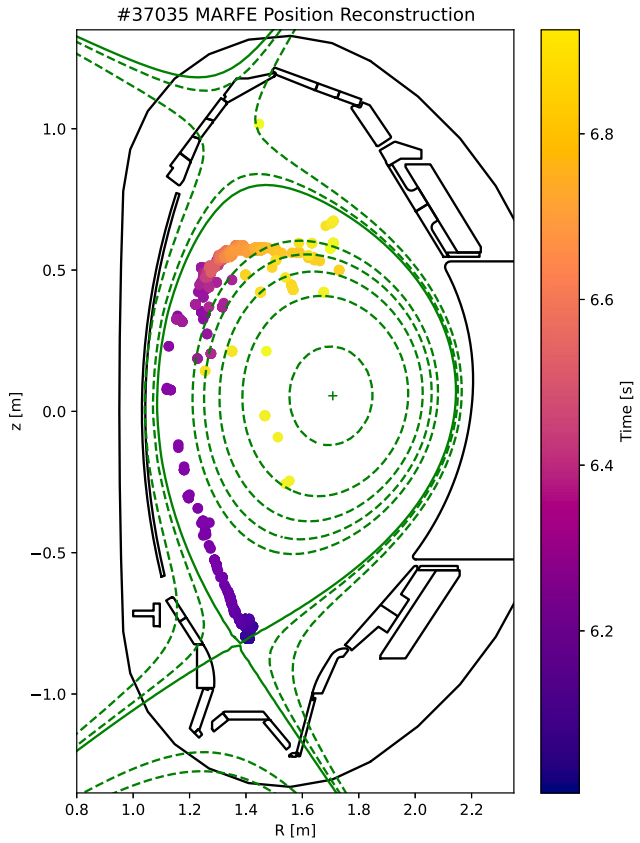

Fig. 2. Offline 2D poloidal XPR/MARFE tracking for ASDEX Upgrade #37035 during a developing HDL with subsequent disruption. The colour of the single points indicate the time during the discharge.

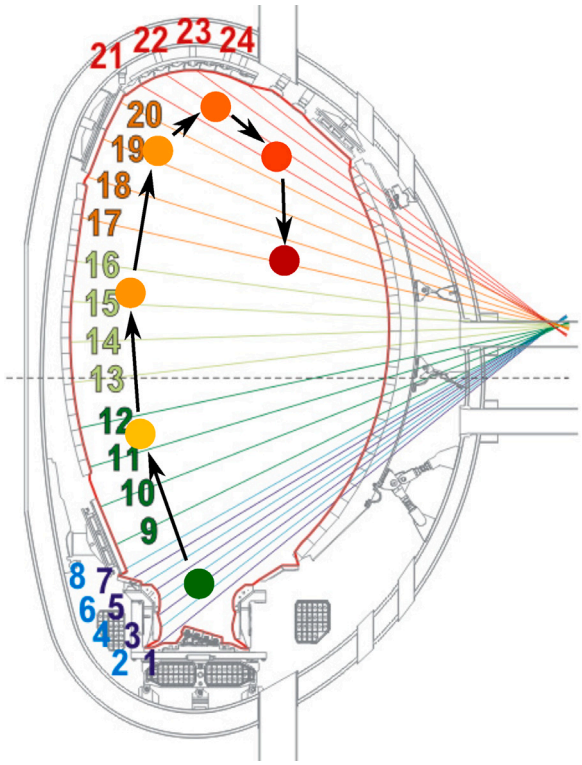

Fig. 3. Poloidal cross section of JET with indicated observation geometry of the horizontal bolometry system KB5H. The coloured dots roughly indicate the XPR/MARFE evolution expected during an HDL. The numbers denote the LOS channel number.

TCV remains a task for future studies, but seems feasible based on the available observations [24].

Due to the availability of real-time bolometry on JET the decision was taken to use the direct observation of the XPR/MARFE for the disruption avoidance experiments.

Fig. 3 illustrates the poloidal observation geometry of the bolometry system KB5H [31] in JET. The system is available to the JET control system in real time with a time resolution of 2 ms. The viewing geometry of the bolometry system is optimized to cover the whole main chamber, with a higher line of sight (LOS) density in the divertor region (LOS 1-8).

Fig. 4 shows the evolution of an XPR/MARFE observed around the switching on of NBI heating in L-Mode. In order to avoid NBI shine through the gas fuelling is increased around 300 ms before the NBI is switched on. This leads to the plasma getting closer to an L-Mode density limit with the development of an XPR/MARFE. The MARFE is moving from the X-Point towards the top of the main chamber (red arrow) and is observable by KB5H during the whole movement. The trajectory of the MARFE roughly corresponds to the green to the dark orange dots illustrated in Fig. 3. After the NBI is switched on the MARFE is moving back down (green arrow) towards the X-Point where finally the XPR disappears and the discharge continues. This observation is common for the way the NBI system is switched on in JET. It shows that the NBI system is suitable to prevent the MARFE to become *critical* and move further into the confined region (red dots in Fig. 3), which would likely initiate a disruption.

The robust peak detection algorithm developed on ASDEX Upgrade [9] has been implemented into the JET Real-Time Central Controller (RTCC2). It proved robust in detecting the position of the XPR/MARFE with sub LOS accuracy. For disruption avoidance the empirical threshold of 5.5 has been chosen, based on *control room experience*. The same observer has been used for detachment control using Argon and Neon seeding in both pure deuterium as well as deuterium tritium experiments during JET DTE3. Here the range in which the controller has been applied was between 3.3–3.7 in numbers of LOS of KL5B.

4. Control system implementation

The implementation of the disruption avoidance schemes varied depending on the devices specific control system capabilities. Due to the different size, age and boundary conditions of the devices the available capabilities were different. It was, however, possible to implement the desired control strategies in all devices.

The control system of TCV is based on MATLAB/Simulink® with a MARTe2 backend [10], which allows rapid development and implementation of new control schemes. Within the WPTE framework the state space observer has been implemented and used for proximity control as well as exception handling [32]. It required the adaption of the calculation of the critical edge electron density (Eq. (2)) to account for the different diagnostic geometry.

The ASDEX Upgrade discharge control system (DCS) is designed to be a distributed control system whose behaviour is defined via configuration [33]. It allows the definition of feedback control modes via configuration and the pulse schedule allows dynamic changes of the control goal based on observed exceptions [34,35]. Both the state space based as well as the XPR/MARFE observer have been implemented to be available to the control system and are now routinely available for experiments. This approach, together with the sufficient length of an ASDEX Upgrade discharge, allowed to provoke and avoid an HDL disruption multiple times within one discharge, allowing more comprehensive scans of the HDL whilst saving experiment time.

For the JET experiments the implementation of the observer has been done using RTCC2 with its MARTe2 backend, using the C++ implementation of the robust peak detection algorithm [9] developed

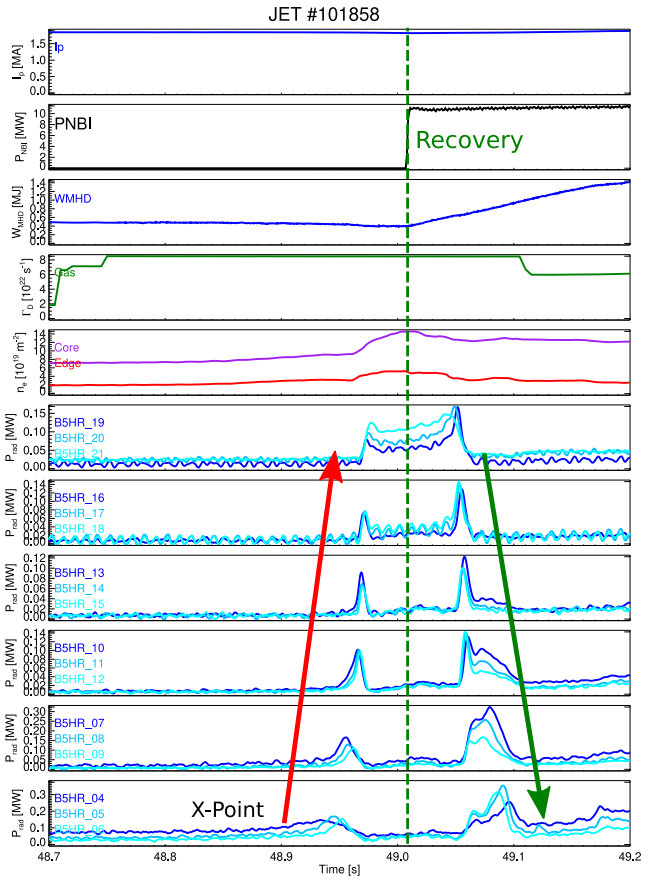

Fig. 4. XPR/MARFE movement in L-Mode before and after application of auxiliary heating. The first plot shows the plasma current, the second the auxiliary heating applied via neutral beam injection (NBI). The stored energy is shown in the third plot. The fourth plot shows the deuterium gas fuelling. The electron density is shown in the fifth plot. The following plots show the intensity of the different bolometry channels of the KB5H system.

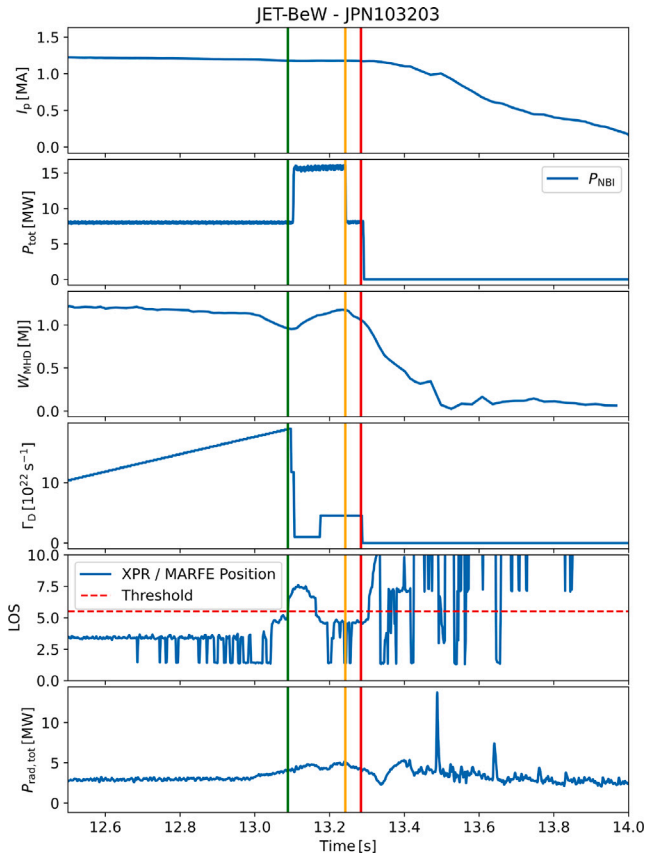

Fig. 5. H-Mode density limit disruption avoidance test on JET-BeW. In the first plot the plasma current is shown. The second plot shows the auxiliary heating applied using NBI. The plasma stored energy is shown in the third plot. The next plot shows the deuterium gas flow. The real-time estimation of the XPR/MARFE position is shown in the fifth plot. The red dashed line indicates the threshold for the disruption avoidance action to be performed. The last plot shows the total radiated power of the plasma. The vertical green line indicates the start of the disruption avoidance action triggered by the XPR/MARFE position exceeding the preset threshold. The orange and red vertical lines indicate the consecutive switching off of the two beam boxes by internal interlocks.

on ASDEX Upgrade. The exception handling was achieved by triggering the so called JTT (JET Termination Time) using the observer from RTCC2 and implementing the feed forward disruption avoidance action into the termination sequence of the pulse which can only be initiated once during the pulse. This did not allow multiple experiments within one discharge, as possible in ASDEX Upgrade, but was sufficient to validate the disruption avoidance scheme.

5. JET: Experimental results

Fig. 5 shows an example of HDL disruption avoidance in JET-BeW with its Beryllium Tungsten wall. The aim of the experiment was to provoke an HDL using a ramp in the applied deuterium gas fuelling. When the XPR/MARFE is detected above the set threshold of 5.5, in numbers of LOS of KB5H, (red dashed line) the disruption avoidance action is triggered (vertical green line). The defined action is the reduction of the gas flow and an increase of the NBI heating power from 8 MW to 16 MW. It has to be noted, however, that the influence of the reduced gas flow is significantly delayed (≈200–300 ms) due to the long travel path [36] of the gas from the valve to the plasma. Therefore, the observed reaction of the disruption avoidance action can dominantly be attributed to the increase of auxiliary heating. The XPR/MARFE movement is stopped at around a LOS number of 7.5 and is moving back towards the X-Point. The plasma stored energy is increasing again until one NBI system after the other (vertical orange and red lines) are turned off due to an internal safety interlock. As a consequence of this the XPR/MARFE is moving back up and the discharge exhibits a *slow* disruption (plasma current quench time > 0.7 s), instead of a proper ramp down.

It is concluded that the disruptive HDL density limit could be avoided in JET using auxiliary heating as actuator. The role of the technical NBI interlocks on the achievable H-Mode density in JET is further discussed in Section 6.

Comparing the XPR/MARFE movement on the different devices it is observed that the time scale on which it occurs increases with increasing size of the device. On JET the movement takes longer as compared to ASDEX Upgrade, where it in turn takes longer as compared to TCV. Currently the observation is only qualitatively and no scaling is available. If this trend holds it is likely that the XPR/MARFE movement in ITER or DEMO will be even slower, but more insight about the dynamics driving the XPR/MARFE movement are required to make predictions.

Comparison to HDL state space

In the following the disruption avoidance experiments performed on JET, with the XPRE/MARFE observer as trigger, are discussed using the empirical HDL state space.

Fig. 6 shows the successful HDL disruption avoidance discharges performed during this work on JET in terms of the empirical HDL state space. Note here that the critical edge density (Eq. (2)) has been

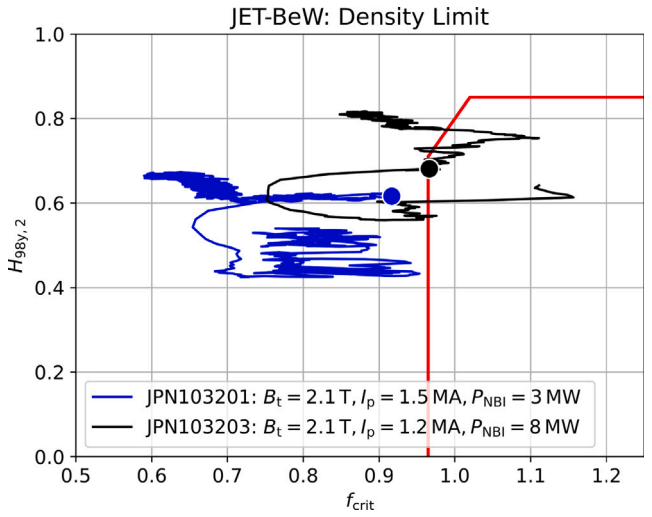

Fig. 6. HDL state space evolution of the HDL in JET. The dots indicate the XPR/MARFE exceeding the set threshold for the disruption avoidance action.

adjusted for the chord length of the edge channel of the interferometer system at JET. JPN103203 (black trajectory) starts at a reasonable H-Mode confinement factor of around 0.8. When the gas flow is increased the critical edge density fraction f_{crit} is increasing whilst the confinement factor is decreasing. The trajectory enters the *critical area* (red border). At $f_{crit} \approx 1.1$ the HL transition is occurring after which both f_{crit} and $H_{98y,2}$ are decreasing together. The black dot indicates the time when the disruption avoidance action is triggered. The fast decrease of $H_{98y,2}$ and f_{crit} are due to the abrupt increase of auxiliary heating. f_{crit} is increasing back to around 0.95 which shows that the density loss due to the HL transition is recovered. After this $H_{98y,2}$ is only slowly increasing until the auxiliary heating is decreased to 8 MW due to the technical interlock. This leads to a further increase of f_{crit} and the consecutive *slow* disruption.

JPN103201 exhibits a similar trajectory as JPN103203. The plasma current is higher compared to JPN103203 and the auxiliary heating is lower. The performance of the discharge is lower from the start, but the initial degradation of the confinement with increasing gas flow is seen. The confinement then stays constant with increasing gas flow and just the f_{crit} is increasing until the XPR/MARFE movement is detected and the disruption avoidance action is triggered. After this the discharge behaves similar as JPN103203.

It is concluded that the disruption avoidance scheme itself is successful in avoiding the HDL disruption at JET. In the presented cases, the consecutive disruptions are caused by the device specific technical limitations present at JET, which do not necessarily apply to future large fusion devices such as ITER or DEMO.

6. Achievable density limit at JET

In this section the influence of technical boundary conditions imposed by the NBI system on the achievable density in JET is discussed. The experiments discussed in Section 5 were significantly hindered by the technical interlocks of the NBI system. During high density operation the neutral density within the NBI beam duct is also increased. This leads to an increase of charge exchange reactions and with this an increased heating of the duct. Both the beam duct pressure and the surface temperature of dump plates can lead to an NBI interlock. Depending on the discharge the reaction to these interlocks can vary. It can trigger a switching off of the deuterium gas flow or a decrease of the NBI heating power, or both.

Fig. 7 shows the discharges performed in previous studies of the H-Mode density limit in JET [17]. Two discharges were compared

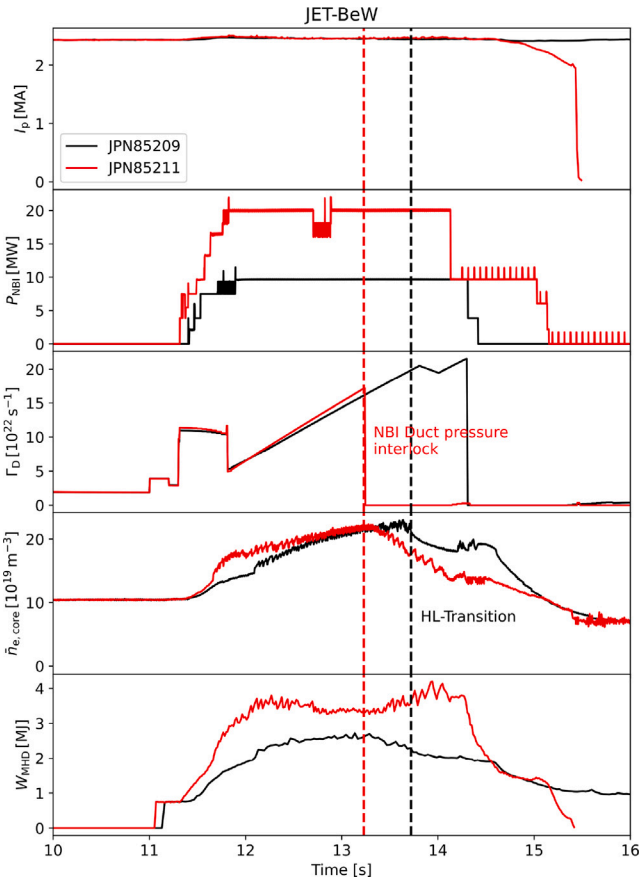

Fig. 7. Trajectories of previous H-Mode density limit experiments in JET. The first plot shows the plasma current. The second plot the applied auxiliary heating via NBI. The deuterium gas flow is shown in the third plot. The fourth plot shows the line averaged core density. The plasma stored energy is shown in the last plot.

with the same toroidal magnetic field and plasma current but different auxiliary NBI heating (JPN85209 (black) with 10 MW and JPN85211 (red) with 20 MW). The aim of the experiments was to achieve an HDL by applying a deuterium gas ramp at constant heating power.

The maximum achieved density in these discharges is indicated with the vertical dashed lines. It is seen that the line averaged core electron density is similar for both discharges. The existing study [17] concludes from this that the achievable electron density in JET has no dependence on the auxiliary power. This is in contrast to the observations made on other devices and also in contrast to what has been observed during this study (see below).

The reason for the maximum achieved in these discharges is, however, different. JPN85209 (black) exhibits a non disruptive HL transition after which the density is decreasing due to the reduction of the confinement time. This is, for example, compatible to the behaviour at ASDEX Upgrade [9]. JPN85211 (red), in contrast, does not reach the HL transition. The confinement is slightly degrading with increasing deuterium gas flow. In this case, the gas flow is switched off due to an NBI duct pressure interlock. After this the discharge is recovering to a Type-I ELMy H-Mode and only disrupts during ramp down due to impurity accumulation.

Fig. 8 shows the evolution of the plasma stored energy W_{MHD} in dependence on the line averaged core electron density $\bar{n}_{e,core}$. Both discharges exhibit an initial increase of the plasma stored energy W_{MHD} with the increasing $\bar{n}_{e,core}$. At some point W_{MHD} saturates and from that point on W_{MHD} starts to decrease with increasing $\bar{n}_{e,core}$. During the gas ramp JPN85209 (black) then exhibits the HL transition after

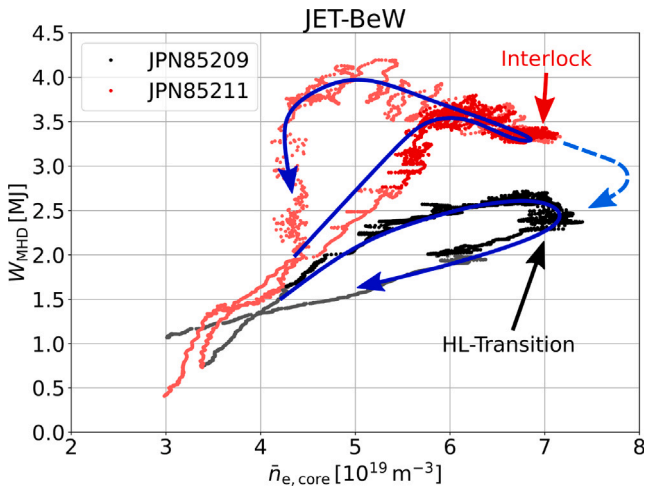

Fig. 8. Time evolution of the plasma stored energy W_{MHD} in dependence of the line averaged core electron density $\bar{n}_{e,core}$. The blue arrows outline the observed time evolution.

which both W_{MHD} and $\bar{n}_{e,core}$ are decreasing. In JPN85211 (red) the degradation of W_{MHD} with increasing $\bar{n}_{e,core}$ continues until the NBI interlock switches off the deuterium gas flow. After this $\bar{n}_{e,core}$ decreases and W_{MHD} is recovering again until the auxiliary heating is reduced from 20 MW to 10 MW.

The dashed light blue arrow indicates the likely trajectory JPN85211 would have taken if the NBI interlock would not have prevented the HL transition. This suggests the actual existence of a dependence of the HDL on the auxiliary heating power which is masked by the technical limitations of the NBI system of JET.

7. Conclusions

Active disruption avoidance for the H-Mode density limit (HDL) has been successfully implemented on ASDEX Upgrade, TCV and JET. Two observers for the onset of the HDL which have been developed at ASDEX Upgrade were migrated to TCV and JET. An empirical *state space* based observer has been used on ASDEX Upgrade and TCV for disruption avoidance using both exception handling as well as proximity control. The second observer, the direct observation of a radiative phenomenon called XPR or MARFE, has been ported from ASDEX Upgrade to JET. It has been used for exception handling based disruption avoidance. The same observer has also been used for detachment control in ASDEX Upgrade and JET DTE3.

All three devices exhibit the HDL in a similar fashion. The XPR/MARFE has a similar development and describes a comparable poloidal movement during the HDL. The time scale on which the HDL is developing appears to be dependent on the size of the device. The HDL progresses slower the larger the device, i.e. it is slower on JET compared to ASDEX Upgrade and in turn it develops slower on ASDEX Upgrade compared to TCV. This would suggest that the development on larger devices such as ITER and DEMO would be even slower compared to todays devices. A prediction of the actual time scales, however, will have to be part of future studies and will require simulation and modelling of the dynamics of the HDL and XPR/MARFE. In addition to this other disruptions paths should be studied and handled in a similar fashion in future work.

CRediT authorship contribution statement

B. Sieglin: Writing – original draft, Software, Methodology, Investigation, Conceptualization. **M. Maraschek:** Methodology, Investigation, Conceptualization. **A. Gude:** Methodology, Investigation, Conceptualization. **F. Klossek:** Investigation. **F. Felici:** Software, Investigation. **M. Bernert:** Methodology, Investigation, Conceptualization. **O. Kudlacek:** Methodology, Investigation. **A. Pau:** Software, Methodology, Investigation, Conceptualization. **L. Piron:** Investigation. **M. Lennholm:** Investigation. **K. Kirov:** Investigation. **S. Hongjuan:** Investigation. **A. Parrott:** Software, Investigation. **P. Fox:** Software, Investigation. **O. Sauter:** Investigation. **C. Stuart:** Software, Investigation. **C. Ashe:** Software, Investigation. **A. Huber:** Investigation. **W. Treutterer:** Software, Investigation.

Declaration of competing interest

The authors declare that they have no known competing financial interests or personal relationships that could have appeared to influence the work reported in this paper.

Acknowledgements

This work has been carried out within the framework of the EUROfusion Consortium, funded by the European Union via the Euratom Research and Training Programme (Grant Agreement No 101052200 — EUROfusion). Views and opinions expressed are however those of the author(s) only and do not necessarily reflect those of the European Union or the European Commission. Neither the European Union nor the European Commission can be held responsible for them.

Data availability

Data will be made available on request.

References

[1] M. Lehnen, K. Aleynikova, P. Aleynikov, D. Campbell, P. Drewelow, N. Eidietis, Y. Gasparyan, R. Granetz, Y. Gribov, N. Hartmann, E. Hollmann, V. Izzo, S. Jachmich, S.-H. Kim, M. Kočan, H. Koslowski, D. Kovalenko, U. Kruezi, A. Loarte, S. Maruyama, G. Matthews, P. Parks, G. Pautasso, R. Pitts, C. Reux, V. Riccardo, R. Roccella, J. Snipes, A. Thornton, P. de Vries, Disruptions in ITER and strategies for their control and mitigation, J. Nucl. Mater. 463 (2015) 39–48, http://dx.doi.org/10.1016/j.jnucmat.2014.10.075, PLASMA-SURFACE INTERACTIONS 21.

[2] B. Esposito, G. Granucci, M. Maraschek, S. Nowak, A. Gude, V. Igochine, E. Lazzaro, R. McDermott, E. Poli, J. Stober, W. Suttrop, W. Treutterer, H. Zohm, D. Brunetti, A.U. Team, Avoidance of disruptions at high βN in ASDEX upgrade with off-axis ECRH, Nucl. Fusion 51 (8) (2011) 083051, http://dx.doi.org/10.1088/0029-5515/51/8/083051.

[3] J. Kim, M.H. Woo, H. Han, Y. In, J.G. Bak, N.W. Eidietis, Integrated Disruption Avoidance and Mitigation in KSTAR, Tech. rep., Japan, 2014, pp. 151–155, URL http://inis.iaea.org/search/search.aspx?orig_q=RN:48068218. PLASMA PHYSICS AND FUSION TECHNOLOGY.

[4] M. Maraschek, A. Gude, V. Igochine, H. Zohm, E. Alessi, M. Bernert, C. Cianfarani, S. Coda, B. Duval, B. Esposito, S. Fietz, M. Fontana, C. Galperti, L. Giannone, T. Goodman, G. Granucci, L. Marelli, S. Novak, R. Paccagnella, G. Pautasso, P. Piovesan, L. Porte, S. Potzel, C. Rapson, M. Reich, O. Sauter, U. Sheikh, C. Sozzi, G. Spizzo, J. Stober, W. Treutterer, Path-oriented early reaction to approaching disruptions in ASDEX Upgrade and TCV in view of the future needs for ITER and DEMO, Plasma Phys. Control. Fusion 60 (1) (2017) 014047, http://dx.doi.org/10.1088/1361-6587/aa8d05.

[5] U. Sheikh, B. Duval, C. Galperti, M. Maraschek, O. Sauter, C. Sozzi, G. Granucci, M. Kong, B. Labit, A. Merle, N. Rispoli, T.T. Team, T.E.M. Team, Disruption avoidance through the prevention of NTM destabilization in TCV, Nucl. Fusion 58 (10) (2018) 106026, http://dx.doi.org/10.1088/1741-4326/aad924.

[6] J. Barr, B. Sammuli, D. Humphreys, E. Olofsson, X. Du, C. Rea, W. Wehner, M. Boyer, N. Eidietis, R. Granetz, A. Hyatt, T. Liu, N. Logan, S. Munaretto, E. Strait, Z. Wang, the DIII-D Team, Development and experimental qualification of novel disruption prevention techniques on DIII-D, Nucl. Fusion 61 (12) (2021) 126019, http://dx.doi.org/10.1088/1741-4326/ac2d56.

[7] B. Sammuli, J. Barr, D. Humphreys, Avoidance of vertical displacement events in DIII-D using a neural network growth rate estimator, Fusion Eng. Des. 169 (2021) 112492, http://dx.doi.org/10.1016/j.fusengdes.2021.112492.

[8] B. Sieglin, M. Maraschek, A. Gude, F. Felici, F. Klossek, O. Kudlacek, P. Lang, A. Pau, B. Ploeckl, W. Treutterer, Dynamic pulse scheduling in ASDEX Upgrade: Disruption avoidance and investigation of the H-Mode density limit, Fusion Eng. Des. 191 (2023) 113546, http://dx.doi.org/10.1016/j.fusengdes.2023.113546.

[9] B. Sieglin, M. Maraschek, A. Gude, F. Klossek, F. Felici, M. Bernert, O. Kudlacek, A. Pau, W. Treutterer, the ASDEX Upgrade Team, the EUROfusion WPTE Team, Disruption avoidance and investigation of the H-Mode density limit in ASDEX Upgrade, Plasma Phys. Control. Fusion 66 (2) (2023) 025004, http://dx.doi.org/10.1088/1361-6587/ad163a.

[10] C. Galperti, F. Felici, T. Vu, O. Sauter, F. Carpanese, M. Kong, G. Marceca, A. Merle, A. Pau, A. Perek, F. Pesamosca, M. Baquero-Ruiz, S. Coda, J. Decker, B. Duval, M. Gospodarczyk, A. Karpushov, S. Marchioni, A. Maier, B. Marletaz, A. Segovia, B. Vincent, C. Yildiz, D. Carnevale, N. Ferron, J. Koenders, B. Kool, G. Manduchi, M. Maraschek, P. Milne, A. Neto, E. Poli, T. Ravensbergen, M. Reich, N. Rispoli, F. Sartori, Overview of the TCV digital real-time plasma control system and its applications, Fusion Eng. Des. 208 (2024) 114640, http://dx.doi.org/10.1016/j.fusengdes.2024.114640.

[11] P. de Vries, M. Johnson, B. Alper, P. Buratti, T. Hender, H. Koslowski, V. Riccardo, JET-EFDA Contributors, Survey of disruption causes at JET, Nucl. Fusion 51 (5) (2011) 053018, http://dx.doi.org/10.1088/0029-5515/51/5/053018.

[12] P.C. de Vries, G. Arnoux, A. Huber, J. Flanagan, M. Lehnen, V. Riccardo, C. Reux, S. Jachmich, C. Lowry, G. Calabro, D. Frigione, M. Tsalas, N. Hartmann, S. Brezinsek, M. Clever, D. Douai, M. Groth, T.C. Hender, E. Hodille, E. Joffrin, U. Kruezi, G.F. Matthews, J. Morris, R. Neu, V. Philipps, G. Sergienko, M. Sertoli, JET EFDA contributors, The impact of the ITER-like wall at JET on disruptions, Plasma Phys. Control. Fusion 54 (12) (2012) 124032, http://dx.doi.org/10.1088/0741-3335/54/12/124032.

[13] P.C. de Vries, J. Rapp, F.C. Schüller, M.Z. Tokar', Partners in the Trilateral Euregio Cluster Collaboration, Influence of recycling on the density limit in TEXTOR-94, Phys. Rev. Lett. 80 (1998) 3519–3522, http://dx.doi.org/10.1103/PhysRevLett.80.3519, URL https://link.aps.org/doi/10.1103/PhysRevLett.80.3519.

[14] J. Rapp, P.D. Vries, F. Schüller, M. Tokar', W. Biel, R. Jaspers, H. Koslowski, A. Krämer-Flecken, A. Kreter, M. Lehnen, A. Pospieszczyk, D. Reiser, U. Samm, G. Sergienko, Density limits in TEXTOR-94 auxiliary heated discharges, Nucl. Fusion 39 (6) (1999) 765, http://dx.doi.org/10.1088/0029-5515/39/6/305.

[15] R. Maingi, M.A. Mahdavi, Review of DIII-D H-mode density limit studies, Fusion Sci. Technol. 48 (2) (2005) 1117–1126, http://dx.doi.org/10.13182/FST05-A1064.

[16] M. Bernert, T. Eich, A. Kallenbach, D. Carralero, A. Huber, P.T. Lang, S. Potzel, F. Reimold, J. Schweinzer, E. Viezzer, H. Zohm, the ASDEX Upgrade team, The H-mode density limit in the full tungsten ASDEX Upgrade tokamak, Plasma Phys. Control. Fusion 57 (1) (2014) 014038, http://dx.doi.org/10.1088/0741-3335/57/1/014038.

[17] A. Huber, S. Brezinsek, G. Sergienko, M. Groth, P. de Vries, L. Aho-Mantila, G. Arnoux, M. Bernert, M. Beurskens, G. Calabro, M. Clever, H. Esser, C. Guillemaut, S. Jachmich, A. Järvinen, C. Linsmeier, G. Matthews, A. Meigs, P. Mertens, V. Philipps, M. Stamp, M. Wischmeier, S. Wiesen, Density limit of H-mode plasmas on JET-ILW, J. Nucl. Mater. 463 (2015) 445–449, http://dx.doi.org/10.1016/j.jnucmat.2014.11.055, PLASMA-SURFACE INTERACTIONS 21.

[18] X. Zheng, J. Li, J. Hu, H. Liu, Y. Jie, S. Wang, J. Li, Y. Duan, M. Li, Y. Li, L. Zhang, Y. Ye, Q. Yang, T. Zhang, Y. Cheng, J. Xu, L. Wang, L. Xu, H. Zhao, F. Wang, S. Lin, B. Wu, B. Lyu, G. Xu, X. Gao, T. Shi, K. He, H. Lan, N. Chu, B. Cao, Z. Sun, G. Zuo, J. Ren, H. Zhuang, C. Li, X. Yuan, Y. Yu, H. Wang, Y. Chen, J. Wu, EAST Team, Density limits investigation and high density operation in EAST tokamak, Plasma Phys. Control. Fusion 58 (5) (2016) 055013, http://dx.doi.org/10.1088/0741-3335/58/5/055013.

[19] A. Huber, M. Bernert, S. Brezinsek, A. Chankin, G. Sergienko, V. Huber, S. Wiesen, P. Abreu, M. Beurskens, A. Boboc, M. Brix, G. Calabrò, D. Carralero, E. Delabie, T. Eich, H. Esser, M. Groth, C. Guillemaut, S. Jachmich, A. Järvinen, E. Joffrin, A. Kallenbach, U. Kruezi, P. Lang, C. Linsmeier, C. Lowry, C. Maggi, G. Matthews, A. Meigs, P. Mertens, F. Reimold, J. Schweinzer, G. Sips, M. Stamp, E. Viezzer, M. Wischmeier, H. Zohm, Comparative H-mode density limit studies in JET and AUG, Nucl. Mater. Energy 12 (2017) 100–110, http://dx.doi.org/10.1016/j.nme.2017.01.005, Proceedings of the 22nd International Conference on Plasma Surface Interactions 2016, 22nd PSI.

[20] U. Stroth, M. Bernert, D. Brida, M. Cavedon, R. Dux, E. Huett, T. Lunt, O. Pan, M. Wischmeier, the ASDEX Upgrade Team, Model for access and stability of the X-point radiator and the threshold for marfes in tokamak plasmas, Nucl. Fusion 62 (7) (2022) 076008, http://dx.doi.org/10.1088/1741-4326/ac613a.

[21] T. Eich, P. Manz, the ASDEX Upgrade team, The separatrix operational space of ASDEX Upgrade due to interchange-drift-Alfvén turbulence, Nucl. Fusion 61 (8) (2021) 086017, http://dx.doi.org/10.1088/1741-4326/ac0412.

[22] M. Giacomin, A. Pau, P. Ricci, O. Sauter, T. Eich, the ASDEX Upgrade team, JET Contributors, the TCV team, First-principles density limit scaling in tokamaks based on edge turbulent transport and implications for ITER, Phys. Rev. Lett. 128 (2022) 185003, http://dx.doi.org/10.1103/PhysRevLett.128.185003.

[23] M. Bernert, F. Janky, B. Sieglin, A. Kallenbach, B. Lipschultz, F. Reimold, M. Wischmeier, M. Cavedon, P. David, M. Dunne, M. Griener, O. Kudlacek, R. McDermott, W. Treutterer, E. Wolfrum, D. Brida, O. Février, S. Henderson, M. Komm, the EUROfusion MST1 team, the ASDEX Upgrade team, X-point radiation, its control and an ELM suppressed radiating regime at the ASDEX Upgrade tokamak, Nucl. Fusion 61 (2) (2020) 024001, http://dx.doi.org/10.1088/1741-4326/abc936.

[24] M. Bernert, S. Wiesen, O. Février, A. Kallenbach, J. Koenders, B. Sieglin, U. Stroth, T. Bosman, D. Brida, M. Cavedon, P. David, M. Dunne, S. Henderson, B. Kool, T. Lunt, R. McDermott, O. Pan, A. Perek, H. Reimerdes, U. Sheikh, C. Theiler, M. van Berkel, T. Wijkamp, M. Wischmeier, The X-Point radiating regime at ASDEX Upgrade and TCV, Nucl. Mater. Energy 34 (2023) 101376, http://dx.doi.org/10.1016/j.nme.2023.101376.

[25] B. Lipschultz, B. LaBombard, E. Marmar, M. Pickrell, J. Terry, R. Watterson, S. Wolfe, Marfe: an edge plasma phenomenon, Nucl. Fusion 24 (8) (1984) 977, http://dx.doi.org/10.1088/0029-5515/24/8/002.

[26] B. Lipschultz, Review of MARFE phenomena in tokamaks, J. Nucl. Mater. 145–147 (1987) 15–25, http://dx.doi.org/10.1016/0022-3115(87)90306-0.

[27] Y. Luo, F. Ding, L. Wang, Y. Duan, T. Ming, S. Mao, Y. Wang, X. Chen, K. Li, D. Ye, L. Meng, J. Xu, T. He, F. Nian, Q. Ma, Z. Hu, Z. Yang, G.-N. Luo, G. Xu, Y. Sun, J. Hu, Investigation of multifaceted asymmetric radiation from the edge (MARFE) with impurity injection from the upper divertor on the experimental advanced superconducting tokamak, Plasma Phys. Control. Fusion 62 (7) (2020) 075005, http://dx.doi.org/10.1088/1361-6587/ab8a62.

[28] M. Mahdavi, T. Osborne, A. Leonard, M. Chu, E. Doyle, M. Fenstermacher, G. McKee, G. Staebler, T. Petrie, M. Wade, S. Allen, J. Boedo, N. Brooks, R. Colchin, T. Evans, C. Greenfield, G. Porter, R. Isler, R.L. Haye, C. Lasnier, R. Maingi, R. Moyer, M. Schaffer, P. Stangeby, J. Watkins, W. West, D. Whyte, N. Wolf, High performance h mode plasmas at densities above the greenwald limit, Nucl. Fusion 42 (1) (2002) 52, http://dx.doi.org/10.1088/0029-5515/42/1/308.

[29] P. Lang, C. Angioni, M. Bernert, A. Bock, T. Engelhardt, R. Fischer, O. Kardaun, B. Ploeckl, M. Prechtl, W. Suttrop, G. Tardini, M. Wischmeier, E. Wolfrum, H. Zohm, ASDEX Upgrade team, H-mode confinement in the pellet-enforced high-density regime of the all-metal-wall tokamak ASDEX Upgrade, Nucl. Fusion 60 (9) (2020) 092003, http://dx.doi.org/10.1088/1741-4326/ab6ea9.

[30] A. Mlynek, L. Casali, O. Ford, H. Eixenberger, ASDEX Upgrade Team, Fringe jump analysis and implementation of polarimetry on the ASDEX Upgrade DCN interferometera), Rev. Sci. Instrum. 85 (11) (2014) 11D408, http://dx.doi.org/10.1063/1.4890574, arXiv:https://pubs.aip.org/aip/rsi/article-pdf/doi/10.1063/1.4890574/13418423/11d408_1_online.pdf.

[31] A. Huber, K. McCormick, P. Andrew, P. Beaumont, S. Dalley, J. Fink, J. Fuchs, K. Fullard, W. Fundamenski, L. Ingesson, F. Mast, S. Jachmich, G. Matthews, P. Mertens, V. Philipps, R. Pitts, S. Sanders, W. Zeidner, Upgraded bolometer system on JET for improved radiation measurements, Fusion Eng. Des. 82 (5) (2007) 1327–1334, http://dx.doi.org/10.1016/j.fusengdes.2007.03.027, Proceedings of the 24th Symposium on Fusion Technology.

[32] T. Vu, F. Felici, C. Galperti, M. Maraschek, A. Pau, N. Rispoli, O. Sauter, B. Sieglin, Integrated real-time supervisory management for off-normal-event handling and feedback control of tokamak plasmas, IEEE Trans. Nucl. Sci. 68 (8) (2021) 1855–1861, http://dx.doi.org/10.1109/TNS.2021.3084410.

[33] W. Treutterer, R. Cole, K. Lüddecke, G. Neu, C. Rapson, G. Raupp, D. Zasche, T. Zehetbauer, ASDEX Upgrade Discharge Control System—A real-time plasma control framework, Fusion Eng. Des. 89 (3) (2014) 146–154, http://dx.doi.org/10.1016/j.fusengdes.2014.01.001, Design and implementation of real-time systems for magnetic confined fusion devices.

[34] W. Treutterer, G. Neu, C. Rapson, G. Raupp, D. Zasche, T. Zehetbauer, Event detection and exception handling strategies in the ASDEX Upgrade discharge control system, Fusion Eng. Des. 88 (6) (2013) 1069–1073, http://dx.doi.org/10.1016/j.fusengdes.2013.03.004, Proceedings of the 27th Symposium On Fusion Technology (SOFT-27); Liège, Belgium, September 24-28, 2012.

[35] B. Sieglin, M. Maraschek, O. Kudlacek, A. Gude, W. Treutterer, M. Kölbl, A. Lenz, Rapid prototyping of advanced control schemes in ASDEX Upgrade, Fusion Eng. Des. 161 (2020) 111958, http://dx.doi.org/10.1016/j.fusengdes.2020.111958.

[36] F. Piccolo, A. Cenedese, D. Ciscato, F. Sartori, Non linear model of the gas introduction module for plasma density control at JET, Fusion Eng. Des. 66–68 (2003) 741–747, http://dx.doi.org/10.1016/S0920-3796(03)00292-8, 22nd Symposium on Fusion Technology.